Mollon, V, Bonhomme, Jorge, Elmarakbi, Ahmed, Arguelles, A and Vina, J (2012) Finite element modelling of mode I delamination specimens by means of implicit and explicit solvers. Polymer Testing, 31 (3). pp. 404-410. ISSN 0142-9418

Downloaded from: http://sure.sunderland.ac.uk/2733/

Usage guidelines

Please refer to the usage guidelines at http://sure.sunderland.ac.uk/policies.html or alternatively contact sure@sunderland.ac.uk.

Polymer Testing 31 (2012) 404–410

Contents lists available at SciVerse ScienceDirect

Polymer Testing

journal homepage: www.elsevier.com/locate/polytest

Property modelling

Finite element modelling of mode I delamination specimens by means of implicit and explicit solvers

V. Mollón [a,*], J. Bonhomme [b], A.M. Elmarakbi [c], A. Argüelles [b], J. Viña [a]

[a] Dept. of Materials Science and Metallurgical Engineering, University of Oviedo, 33203 Gijón, Spain
[b] Dept. of Construction and Manufacturing Engineering, University of Oviedo, 33203 Gijón, Spain
[c] School of Computing and Technology, University of Sunderland, Sunderland SR6 0DD, United Kingdom

ARTICLE INFO

Article history:
Received 6 November 2011
Accepted 17 December 2011

Keywords:
Polymer-matrix composites
Delamination
Fracture
Finite element analysis (FEA)
Cohesive zone model
Two-step extension method

ABSTRACT

The simulation of delamination using the Finite Element Method (FEM) is a useful tool to analyse fracture mechanics. In this paper, simulations are performed by means of two different fracture mechanics models: Two Step Extension (TSEM) and Cohesive Zone (CZM) methods, using implicit and explicit solvers, respectively.

TSEM is an efficient method to determine the energy release rate components G_{Ic}, G_{IIc} and G_{IIIc} using the experimental critical load (P_c) as input, while CZM is the most widely used method to predict crack propagation (P_c) using the critical energy release rate as input.

The two methods were compared in terms of convergence performance and accuracy to represent the material behaviour and in order to investigate their validity to predict mode I interlaminar fracture failure in unidirectional AS4/8552 carbon fibre composite laminates.

The influence of increasing the loading speed and using mass scaling was studied in order to decrease computing time in CZ models.

Finally, numerical simulations were compared with experimental results performed by means of Double Cantilever Beam specimens (DCB).

Results showed a good agreement between both FEM models and experimental results.

© 2011 Elsevier Ltd. All rights reserved.

1. Introduction

Delamination failure (separation of two adjacent plies in composite laminates) is frequently found in composite structures. This kind of damage is considered one of the most critical in laminated fibre reinforced composites.

The delamination crack may propagate undetected during inspection under the action of static or dynamic loads. It can lead to the ultimate failure of the component, inducing reduction in stiffness and compressive load-carrying capacity of a structure. Consequently, the analysis of the onset and propagation of the delamination continues to be studied by composite technology researchers.

The delamination process is characterized by means of the energy release rate (G), which is a measurement of the energy lost in the test specimen per unit of specimen width for an infinitesimal increase in delamination length. In mathematical form:

$$G = -\frac{1}{B}\frac{dU}{da} \tag{1}$$

The onset of delamination takes place when G reaches a critical value G_c.

Finite Element (FE) analysis is a numerical procedure commonly used to determine G_c in engineering problems involving delamination failure. There are several mathematical models developed in the scientific literature in order to compute G_c and to predict crack propagation for different loading modes by means of FE codes. Among

* Corresponding author. Tel.: +34 647488611.
E-mail address: mollonvictoria@uniovi.es (V. Mollón).

0142-9418/$ – see front matter © 2011 Elsevier Ltd. All rights reserved.
doi:10.1016/j.polymertesting.2011.12.008

these methods, the Virtual Crack Closure Technique (VCCT) and the Cohesive Zone Model (CZM) are extensively used.

The CZM method presents fracture as a gradual phenomenon in which separation takes place across a cohesive zone. Some of the first works in this field can be attributed to Dugdale [1] and Barreblatt [2]. The crack onset and growth will take place when the forces at the cohesive zone overcome the cohesive tractions. Thus, cohesive zone elements are used to describe the cohesive behaviour between plies. Cohesive zone models are particularly attractive when interfacial strengths are relatively weak compared with the adjoining material, as is the case in composite laminates [3].

CZM is available in all important commercial FE packages. Nevertheless, CZM models sometimes present convergence problems with implicit solvers, so this model is usually used with explicit solvers. This is because most implicit solvers are not so efficient with discontinuous functions.

It is also well known that explicit calculations with CZM show spurious oscillations of computed forces leading to undesirable results [4,5]. This problem is caused by an instability which occurs just after the stress reaches the peak strength of the interface. This problem can be controlled by techniques such as using a very fine mesh which, on the other hand, leads to very high computational time. Other authors have proposed artificial damping methods with additional energy dissipations such as those proposed by Gao and Bower [6]. Some authors have developed cohesive models specially designed to overcome this problem. For example, Hu et al. [7] have developed a model termed Adaptive Cohesive Model (ACM) with a pre-softening zone ahead of the existing traditional softening zone. In this zone, the initial stiffness and the interface strengths at the integration points of cohesive elements are gradually reduced as the relative displacements at these points increase.

Regarding implicit solvers, the most extended method to solve delamination problems is the VCCT method [8] which was first formulated by Rybicki and Kanninen [9]. This method has been successfully used to predict delamination initiation in flat laminates with an embedded delamination [10]. The VCCT model has evolved from the Finite Crack Extension Method and the Virtual Crack Extension Method [11] and is based on Irwin's crack closure integral [12].

In this work the Two Step Extension Method (TSEM) has been used as an alternative to the VCCT method. The TSEM is based on the calculation of the forces and displacement at the crack tip in two steps. Irwin's formulation is applied without any simplification [12,13]. Other studies have demonstrated that TSEM is a good candidate, similar to VCCT, to model the delamination process [14].

In this paper, mode I delamination tests have been modelled by means of TSEM (implicit solver) and CZM (explicit solver) in order to compare both procedures. Finally, an experimental program has been performed in order to obtain G_{Ic} experimentally by means of Double Cantilever Beam (DCB) specimens. Numerical results were compared with experimental results in order to demonstrate the validity of both methods in terms of convergence performance and accuracy to represent the material delamination behaviour.

2. Experimental and numerical methods

2.1. Experimental procedure

Five samples of Hexcel AS4/8552 laminates were tested in mode I interlaminar fracture test following the ASTM Standard D 5528-01 [15]. This material is a unidirectional carbon fibre-epoxy composite that has been modified in order to improve toughness. Table 1 shows the mechanical properties of this laminate. Fig. 1 shows the DCB specimen.

As it can be seen in Fig. 1, opening forces are applied to the Double Cantilever Beam (DCB) specimens to produce mode I delamination fracture. The DCB specimen is composed of 32 unidirectional plies and it contains a non-adhesive insert at the midplane to act as a delamination starter. The structure of the laminates was [0°_{16}/insert/0°_{16}].

The DCB specimen was 150 mm in total length, 50 mm in crack length, 25 mm width and 6 mm thickness (nominal dimensions).

The specimens were tested on a MTS testing machine with a 5 kN load cell, applying a constant displacement velocity of 1 mm/min. The load-displacement response was obtained and a travelling optical microscope (100×) was used to measure the crack length during the test.

The Modified Beam Theory (MBT) Eq. (2) and the Compliance Calibration (CC) Eq. (3) data reduction methods were used to calculate the strain energy release rate, G_{Ic}:

$$G_{Ic} = \frac{3P_C\delta}{2B(a+|\Delta|)} \tag{2}$$

$$G_{Ic} = \frac{nP\delta}{2Ba} \tag{3}$$

where P_c is the critical load, δ, B, h and a are the load point displacement, specimen width, specimen thickness and delamination length respectively while Δ and n are calibration parameters [15].

According to ASTM Standard D 5528-01 [15], the critical value of P (P_c) is calculated from the load-displacement curve (see Fig. 2) as the onset of the crack growth. This parameter may be calculated as the point of deviation from linearity (*NL*), the point at which delamination is visually observed (*VIS*) and the point at which the compliance has increased by 5% or the load has reached a maximum value (5%/*max*).

Table 1
Laminate mechanical properties.

Property (MPa)	AS4/8552
E_{11} (Longitudinal elastic modulus)	144,000
E_{22} (Transversal elastic modulus)	10,600
G_{12} (Shear elastic modulus)	5360
σ_{11} (Longitudinal tensile strength)	1703
σ_{22} (Transversal tensile strength)	30.8
σ_s (Shear strength)	67.7

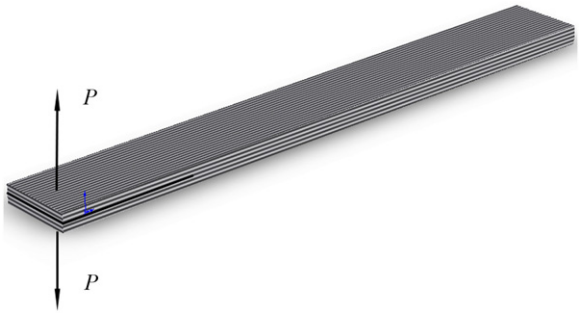

Fig. 1. DCB specimen.

2.2. Numerical methods

In this work, simulations of mode I interlaminar fracture toughness tests of composite material were conducted by means of two different fracture mechanics methods: Two Step Extension and Cohesive Zone methods, using ANSYS® (implicit) and LS-DYNA® (explicit) packages respectively.

2.2.1. Two Step Extension Method

In this numerical method, the crack path is modelled using pairs of coincident nodes. The forces at the crack tip are calculated in a first step when the load reaches the critical value. The imposed displacement in the sample is then held and the coupled DOFs (degrees of freedom) of the nodes at the crack tip are released in a second step. Displacements are then calculated in this second step (see Fig. 3a and b).

This procedure can be analytically described as follows:

$$G_I = \frac{1}{2B\Delta a}\sum_{i=1}^{n} F_{y1i}(v_{1i} - v_{1'i}) \tag{4}$$

$$G_{II} = \frac{1}{2B\Delta a}\sum_{i=1}^{n} F_{x1i}(u_{1i} - u_{1'i}) \tag{5}$$

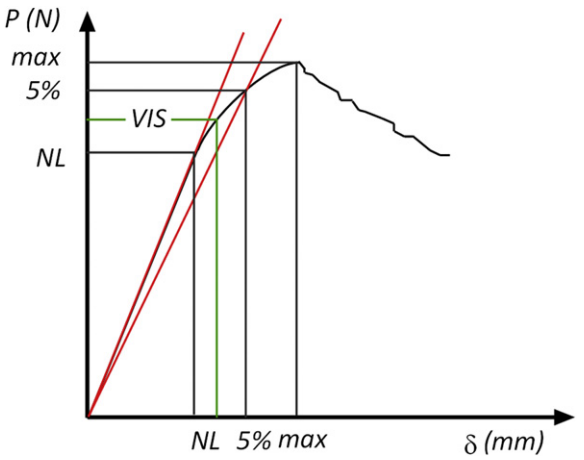

Fig. 2. Mode I test. Critical load calculation.

$$G_{III} = \frac{1}{2B\Delta a}\sum_{i=1}^{n} F_{z1i}(w_{1i} - w_{1'i})$$

where:

- *B:* sample width
- Δa*:* crack length increment
- v_{1i}: vertical displacement of nodes at the crack tip
- u_{1i}: horizontal displacement of nodes at the crack tip
- F_{y1i}: vertical nodal force at the crack tip
- F_{x1i}: horizontal nodal force at the crack tip *x*-axis
- F_{z1i}: horizontal nodal force at the crack tip *z*-axis

The suffix *i* takes into account the extension to a 3D system, where *n* nodes are placed along the crack front.

The DCB specimens were modelled by means of four node 2D solid elements in plane strain with two degrees of freedom at each node (translations in the nodal *x* and *y* directions). The element length was set to 0.33 mm near the crack tip, so the ratio of the crack increment length over the initial crack length was $\Delta a/a_0 = 0.0066$. Fig. 4 shows the final mesh used to perform the calculations. G_{Ic} was calculated by means of Eq. (4). Finite element calculations were performed by means of an ANSYS® implicit package.

Material behaviour was implemented as transversely isotropic (i.e. the mechanical properties perpendicular to the laminate plane, have been made equal to the in-plane transversal properties).

2.2.2. Cohesive Zone Method (CZM)

These calculations were performed by means of LS-DYNA® explicit software.

The main solution methodology is based on explicit time integration. This code is one of the most widely used to model impact and crash situations in layered composites. Cohesive elements are implemented in the code.

In this method, the delamination surface is modelled between individual laminas by *interface elements* of cohesive strengths which exhibit the approximate behaviour of delamination cracks (see Fig. 5).

Compared to VCCT, CZM has the advantage of being able to predict the onset and propagation of a crack without the need to implement a pre-existing crack [16].

The combined effects of the damage processes are well defined by unique models called Cohesive Zone Models. By implementing these models, one may take the delamination into account by finite element analysis.

In a cohesive element, a maximum opening normal stress is associated with an initial crack opening and a maximum crack length is associated with zero bond strength (see Fig. 6).

The fracture toughness of the bond between plies (a material input) is equal to the integral of the element traction versus crack opening.

$$G_{Ic} = \int_0^{\delta_I^F} \sigma d\delta \tag{6}$$

One of the most widely used constitutive equations is the bilinear law [17] as shown in Fig. 6. The initial slope

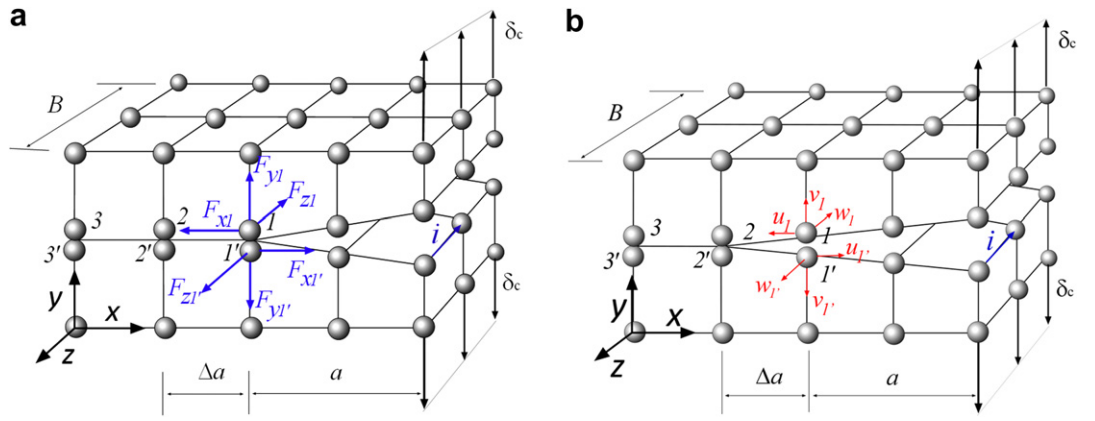

Fig. 3. a) DOFs at coincident nodes are coupled. The corresponding forces are computed. (b) DOFs of the nodes at the crack front are released. The corresponding displacements are computed.

of the curve is the penalty stiffness (k). This value is usually high in order to reproduce the crack behaviour. In pure modes I or II, when the normal or shear traction reach the critical value (σ^0 or τ^0) the stiffness is progressively reduced to zero.

The discontinuity at maximum load shown by the bilinear law can be avoided by means of a smooth nonlinear law (Fig. 7).

Different laws developed in the scientific literature can be reviewed in Ref. [18].

In a real structure, more than one pure load mode is usually present at the crack front, so it is necessary to define a general formulation for mixed mode delamination.

For pure modes I and II, the onset of delamination can be determined by comparing G_I or G_{II} with their critical values (G_{Ic} or G_{IIc}).

However, under mixed mode loading, the onset of delamination may occur before any of the energy release rate values reach their respective critical values.

There are several failure criteria developed in the scientific literature for the onset of delamination as the Power Law [19–21] and the Benzeggagh and Kenane [22] Law.

Nevertheless, in this work this issue is not relevant as only pure mode I is developed in DCB specimens.

The DCB model was performed by two beams or sub-laminates. Every sub-laminate was modelled by means of fully integrated S/R-8 node solid elements, with two elements across the thickness. Material behaviour was simulated as orthotropic by means of the MAT_002 (*MAT_ORTHOTROPIC_ELASTIC) option.

On the other hand, a cohesive interface was performed between the beams with one element across the thickness. The cohesive element thickness was 0.01 mm. This layer was implemented by means of the MAT_138 (*MAT_COHESIVE_MIXED_MODE) model, based on the bilinear law. This option requires the independent material parameters shown in Table 2.

G_{Ic} and G_{IIc} values have been obtained from previous numerical studies [23]. There is no general agreement in the scientific literature about the stiffness of the cohesive zone and interfacial strength s for carbon/epoxy composites. Turon et al. [24] have proposed the following equation to calculate the interfacial stiffness:

$$k = \frac{\alpha E_3}{t} \tag{7}$$

where $\alpha \gg 1$ (Turon et al. proposed $\alpha > 50$), E_3 is the transverse elastic modulus and t the sublaminate thickness. Other authors have proposed values between 10^4 and 10^7 [25,26]. Regarding the interfacial strength, Alfano and Crisfield [27] have found that variations in this parameter do not affect too much the final results, and a decrease in the interfacial strength tended to improve convergence. Even more, the reduction of the interfacial strength has the effect of enlarging the cohesive zone so the softening behaviour ahead the crack tip could be better captured for a given mesh [24].

In this work, a value of $k_I = k_{II} = 3 \times 10^4$ and $\sigma^0 = 45$ MPa has been taken according to [7].

The mode mixity is defined as:

$$\beta = \frac{\delta_{II}}{\delta_I} \tag{8}$$

In this model, the mixed mode damage initiation displacement (δ_m^0) is given by:

$$\delta_m^0 = \delta_I^0 \delta_{II}^0 \sqrt{\frac{1+\beta^2}{\left(\delta_{II}^0\right)^2 + \left(\beta \delta_I^0\right)^2}} \tag{9}$$

where δ_I^0 and δ_{II}^0 are the single mode damage initiation separations:

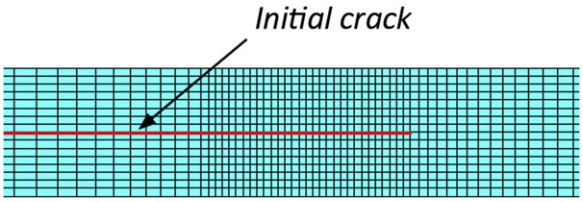

Fig. 4. Mesh for TSE model near the crack tip.

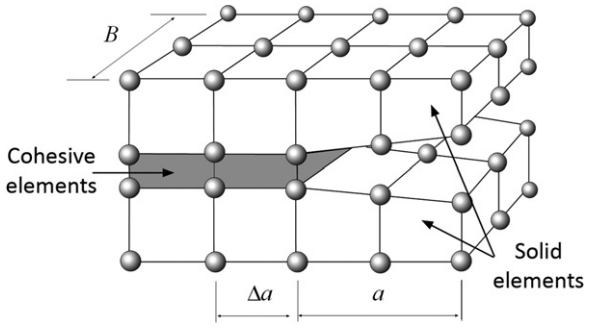

Fig. 5. Cohesive model.

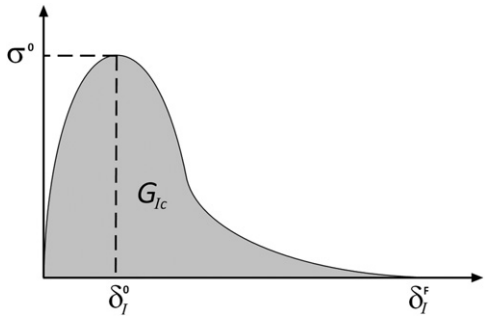

Fig. 7. Smooth nonlinear law.

$$\delta_I^0 = \frac{\sigma^0}{k_I} \tag{10}$$

$$\delta_{II}^0 = \frac{\tau^0}{k_{II}} \tag{11}$$

The cohesive element fails when the ultimate mixed mode displacement (δ_m^F) is reached.

Two alternative formulations are implemented for MAT_138:

The Power Law (for values of $\eta > 0$):

$$\delta_m^F = \frac{2(1+\beta)^2}{\delta_m^0}\left[\left(\frac{\sigma^0}{G_{Ic}}\right)^{\eta} + \left(\frac{\tau^0\beta^2}{G_{IIc}}\right)^{\eta}\right]^{\frac{-1}{\eta}} \tag{12}$$

The Benzeggagh-Kenane Law: (for values of $\eta < 0$):

$$\delta_m^F = \frac{2}{\delta_m^0\left(\frac{1}{1+\beta^2}\sigma^0 + \frac{\beta^2}{1+\beta^2}\tau^0\right)} \cdot \left[G_{Ic} + (G_{IIc} - G_{Ic}) \cdot \left(\frac{\beta^2\tau^0}{\sigma^0 + \beta^2\tau^0}\right)^{|\eta|}\right] \tag{13}$$

In this work, the power law with $\eta = 1$ has been used. As stated before, in DCB tests only pure mode I takes place at the crack tip, so these parameters are not so relevant.

Several models were performed in order to obtain a successful FEM simulation.

First of all, the element size in the different parts of the model had to be set. As is well known, the usage of small elements gives rise to a more accurate solution. Nevertheless, as element number increases the total CPU time to solve the problem increases. This effect is particularly important with explicit solvers where the critical time step depends on the dimensions of the smallest element. In this way, the selection of the gap thickness between both sublaminates (cohesive element thickness) must be also carefully fixed.

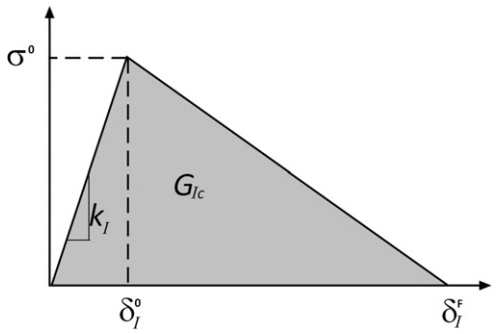

Fig. 6. Mode I bilinear law.

In this work, a previous study was developed in order to determine the optimum size of the elements in the cohesive zone ahead of the crack front in order to optimize the CPU time while maintaining the accuracy of the results. It was found out that cohesive element length about 2 mm near the crack front was small enough to obtain results with a good approximation to the experimental values and leads to a reasonable computational cost. The final mesh density used in the subsequent runs is shown in Fig. 8.

3. Results and discussion

3.1. Experimental results

Five specimens were tested following the experimental procedure described in point 2.1. Experimental curves were linear up to failure, so the critical load was taken as the maximum load. Table 3 shows the critical load (P_c) and displacement (δ_c) obtained in the experimental tests. This table also shows the energy release rate G_{Ic} calculated by means of MBT and CC procedures. The CC reduction method has been selected as a reference for subsequent comparisons as this was the procedure that gave the lowest standard deviation. The coefficient of variation (CV) of the experimental results was 11%. Other authors have found

Table 2
Cohesive parameters.

	Symbol	LS-DYNA parameter	Value
Initial stiffness in mode I	k_I	*EN*	3×10^4 N/mm
Initial stiffness in shear	k_{II}	*ET*	3×10^4 N/mm
Mode I critical energy release rate	G_{Ic}	*GIC*	0.250 N.mm/mm^2
Mode II critical energy release rate	G_{IIc}	*GIIC*	0.791 N.mm/mm^2
Peek traction in mode I	σ^0	*T*	45 N/mm^2
Peek traction in mode II	τ^0	*S*	45 N/mm^2
Mixed mode parameter	η	*XMU*	1

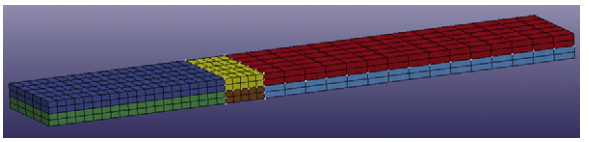

Fig. 8. Mesh used in the explicit analysis.

similar experimental dispersion in interlaboratory round robin tests [28].

3.2. Numerical results

3.2.1. Two-Step Extension Method

Each experimental specimen tested as described in 3.1 was modelled by means of an ANSYS® package. Each model was prepared as stated in 2.2.1 and loaded with the corresponding experimental load shown in Table 3. The Two Step Extension Method was used as described in 2.2.1 in order to calculate the critical energy release rate. The results obtained in these runs can be seen in Table 4.

As we can see comparing Tables 3 and 4, there is good agreement between experimental results and ANSYS® runs as the difference between G_{Ic} mean values obtained from both procedures were of the order of 5%. This error is low, taking into account the observed experimental dispersion.

3.2.2. Cohesive Zone Method (CZM)

As the experimental tests were performed at low velocity (1 mm/min = 0.017 mm/s), the experimental time to maximum load was about 1.5 min. This time is too long for explicit software, resulting in very high computational cost. In order to reduce the computing time, two strategies can be used. On one hand, the loading speed can be increased. On the other hand, mass scaling can be applied for the lowest velocities. In both cases a sensitivity study must be developed in order to assess the validity and accuracy of the results.

In this work, the influence of the loading speed on the critical load has been studied in order to prove the validity of increasing that parameter. Mass scaling was also used to obtain faster solutions with the lowest velocities.

Mass scaling refers to a technique whereby non-physical mass is added to a structure in order to achieve a larger explicit time step. Mass scaling reduces the simulation time, but it may affect the results. This procedure is justifiable when the effect on the results is negligible. This is the case of quasi-static analysis where the velocity is low and so the kinetic energy is very small relative to the peak internal energy [29]. The effect of the mass scaling can be addressed changing this parameter and observing the sensitivity on the obtained results.

Table 3
Experimental results.

Specimen	Critical load (N)	Critical displacement (mm)	G_{Ic} (J/m^2) (MBT)	G_{Ic} (J/m^2) (CC)
1	138.0	1.47	267.88	266.28
2	130.6	1.73	293.67	281.91
3	167.0	1.41	352.78	318.24
4	123.2	1.50	247.71	238.76
5	134.1	1.51	275.79	265.83
Mean (x)	138.6	1.52	287.6	274.2
Standard deviation (s)	16.8	0.12	40.0	29.1

Table 4
TSEM results.

Specimen	G_{Ic} (J/m^2)
1	242.6
2	259.9
3	341.3
4	227.2
5	226.0
Mean (x)	259.4
Standard deviation (s)	47.8

Table 5
Influence of the loading speed on the results.

Velocity (mm/s)	Mass Scale	P_c (N)
0.25	-5×10^{-6}	137.7
0.50	-5×10^{-6}	138.7
5	-5×10^{-7}	137.7
10	-5×10^{-7}	137.8
100	0	138.7
200	0	137.9

The critical loads (P_c) obtained in these runs are shown in Table 5. The mass scaling factors shown in this table have been selected in order to reduce CPU time without having any significant influence on the results.

As can be seen in Table 5, P_c remains almost constant for loading speeds up to 100–200 mm/s.

This means that, when simulating a quasi-static mode I test, the loading speed can be increased from quasi-static values up to about 100 mm/s in order to speed up the solution procedure, without affecting the accuracy of results.

Following these results, the critical load obtained with the lowest velocity (0.25 mm/s) was taken as quasi-static and used to compare with the experimental and TSEM methods. Good agreement was found between experimental and CZM models (see Tables 3 and 5) as the difference between critical loads were in the order of 1% (P_{cexp} = 138.6 N/P_{cCZM} = 137.7 N) (see Fig. 9).

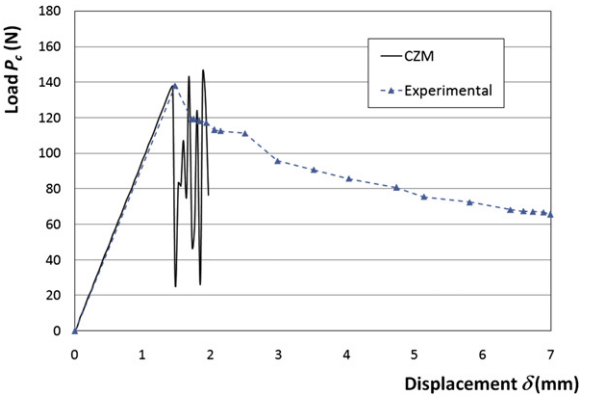

Fig. 9. Experimental and CZM load-displacement curves.

As can be seen in Fig. 9, the CZM curve shows linear behaviour up to maximum load. As stated before, at this point instabilities began to occur due to the suddenly change in stiffness after the stress reaches the peak strength of the interface. This behaviour is not relevant for this study as only results at maximum load are compared.

In order to study the propagation behaviour by means of CZM, other procedures should be implemented in LS-DYNA® as smooth traction-separation laws or the adaptive cohesive model (ACM) with pre-softening zone [7]. By using these methods, smooth propagation behaviour would be obtained.

4. Conclusions

The TSEM is a very efficient method to work with implicit solvers. It is easy to implement and useful to support experimental results. This method, as presented in this work, uses as input the critical load obtained from experimental results and furnishes the energy release rate G_{Ic} G_{IIc} and G_{IIIc} in a generalized load state by means of simple calculations. Regarding the accuracy of the method, good agreement was found between experimental and numerical results as errors between both procedures were below 5%.

On the other hand, CZM running on explicit solvers also furnishes very accurate results (the critical loads obtained from experimental and numerical results differs only by 1%). This method is very useful to study the onset and propagation of cracks. The material model uses the critical energy release rate obtained in pure modes I, II and III as input parameters and furnishes the critical load needed to initiate or propagate the crack. Nevertheless, in order to reduce CPU times in quasi-static tests, some issues must be taken into account, such as introducing mass scaling and increasing the loading speed. These parameters should be carefully adjusted to avoid any influence on the results.

It was found that the loading speed can be increased up to 100–200 mm/min with no significant influence on the obtained results, on the other hand, mass scaling of the order of 5×10^{-7} was successfully used with the lowest velocities to decrease computing time.

If the critical load is known, the TSE method is better than CZM to analyse and solve mixed mode problems. This is because the decomposition of modes is directly obtained without the need of any criterion, via Eqs. (4)–(6) and the solution is more stable near the maximum load. Nevertheless, if the critical energy release rates in pure modes I and II are known and the critical load unknown, the preferred method to calculate the initiation (critical load) and crack propagation would be the CZM.

Finally, if crack propagation needs to be studied, any action should be taken in order to avoid spurious oscillations after maximum load as implementing a smooth law or an adaptative cohesive model.

References

[1] D. Dugdale, Yielding of steel sheets containing slits, J. Mech. Phys. Sol. 8 (1960) 100–104.
[2] G. Barenblatt, The mathematical theory of equilibrium cracks in brittle fracture, Adv. Appl. Mech. 7 (1962) 55–129.
[3] A. Needleman, An analysis of intersonic crack growth under shear loading, J. Appl. Mech. 66 (1999) 847–857.
[4] Y. Mi, M.A. Crisfield, G.A.O. Davis, Progressive delamination using interface element, J. Comp. Mat. 32 (1998) 1246–1272.
[5] J.P.M. Goncalves, P.M.S.T. De Castro, A.T. Marques, Interface element including point-to-surface constraints for three-dimensional problems with damage propagation, Eng. Comput. 17 (2000) 28–47.
[6] Y.F. Gao, A.F. Bower, A simple technique for avoiding convergence problems in finite element simulations of crack nucleation and growth on cohesive interfaces, Model. Simul Mat. Sci. Eng. 2 (2004) 453–463.
[7] N. Hu, Y. Zemba, T. Okabe, C. Yan, H. Fukunaga, A.M. Elmarakbi, A new cohesive model for simulating delamination propagation in composite laminates under transverse loads, Mech. Mater. 40 (2008) 920–935.
[8] R. Krueger, Virtual crack closure technique. History, approach and applications, Appl. Mech. Rev. 57 (2004) 109–143.
[9] E.F. Rybicki, M.F. Kanninen, Finite element calculation of stress intensity factors by a modified crack closure integral, Eng. Fract. Mech. 9 (4) (1977) 931–938.
[10] Z. Mikulik, B.G. Prusty, R.S. Thomson, D.W. Kelly, Application of Fracture Mechanics-Based Methodologies for Failure Predictions in Composite Structures, Conference on Damage in Composite Materials Stuttgart (2006).
[11] T.K. Hellen, On the method of virtual crack extension, Int. J. Num Meth Eng. 9 (1) (1975) 187–207.
[12] G.R. Irwin, I. Fracture, in: S. Flüge (Ed.), Handbuch der Physik, Springer-Verlag, New York, 1958.
[13] R. Krueger, The Virtual Crack Closure Technique: History, Approach and Applications NASA/CR-2002-211628. ICASE Report No. 2002-10. Hampton, Virginia (2002).
[] V. Mollón, J. Bonhomme, J. Viña, A. Argüelles, Theoretical and experimental analysis of carbon epoxy asymmetric dcb specimens to characterize mixed mode fracture toughness, Polym. Test. 29 (2010) 766–770.
[15] Mode I Interlaminar Fracture Toughness of Unidirectional Fibre-reinforced Polymer Matrix Composites, ASTM D 5528-01, 2007, e3.
[16] D. Xie, A.M. Waas, Discrete cohesive zone model for mixed-mode fracture using finite element analysis, Eng. Fract. Mech. 73 (2006) 1783–1796.
[17] P. Camanho, C.G. Dávila, Mixed-mode Decohesion Finite Elements for the Simulation of Delamination in Composite Materials NASA/TM-2002-211737, Langley Research Centre Hampton, Virginia, 2002.
[18] C. Shet, N. Chandra, Analysis of energy balance when using cohesive zone models to simulate fracture processes, J. Eng. Mater. Tech. 124 (4) (2002) 440–450.
[19] P.P. Camanho, F.L. Matthews, Delamination onset prediction in mechanically fastened joints in composite laminates, J. Comp. Mater. 33 (10) (1999) 906–927.
[20] C.G. Dávila, E.R. Johnson, Analysis of delamination initiation in postbuckled dropped-ply laminates, AIAA J. 31 (4) (1993) 721–727.
[21] W. Cui, M.R. Wisnom, M. Jones, A comparison of failure criteria to predict delamination of unidirectional glass/epoxy specimens waisted through the thickness, Composites 23 (3) (1992) 158–166.
[22] M.L. Benzeggagh, M. Kenane, Measurement of mixed-mode delamination fracture toughness of unidirectional glass/epoxy composites with mixed-mode bending apparatus, Comp. Sci. Tech. 56 (1996) 439–449.
[23] J. Bonhomme, A. Argüelles, J. Viña, I. Viña, V. Mollón, Compliance correction for numerical and experimental determination of mode I and mode II composite fracture failure, Mech. Adv. Mater. St. 17 (2010) 377–381.
[24] A. Turon, C.G. Dávila, P.P. Camanho, J. Costa, An engineering solution for mesh size effects in the simulation of delamination using cohesive zone models, Eng. Fract. Mech. 74 (2007) 1665–1682.
[25] P.P. Camanho, C.G. Dávila, M.F. de Moura, Numerical simulation of mixed-mode progressive delamination in composite materials, J. Comp. Mater. 37 (16) (2003) 1415–1438.
[26] Z. Zou, S.R. Reid, S. Li, P.D. Soden, Modelling interlaminar and intralaminar damage in filament wound pipes under quasi-static indentation, J. Comp. Mater. 36 (2002) 477–499.
[27] G. Alfano, M.A. Crisfield, Finite element interface models for the delamination analysis of laminated composites: mechanical and computational issues, Int. J. Num. Meth. Eng. 77 (2) (2001) 111–170.
[28] T.K. O'Brien, R.H. Martin, Round robin testing for mode I interlaminar fracture toughness of composite materials, J. Comp. Tech. Res. 15 (4) (1993) 269–281.
[29] www.dynasupport.com, Quasi-static simulations.